

1 **Title: Influences of local and global context on local orientation perception**

2 **Running title: Influences of local and global context**

3 **Jinfeng Huang<sup>#,a,b,c</sup>, Yifeng Zhou<sup>b,c</sup>, Tzvetomir Tzvetanov<sup>#,b,d,e</sup>**

4 <sup>a</sup> current affiliation: Department of Psychology, Hebei Normal University,  
5 Shijiazhuang, P.R.China.

6 <sup>b</sup> Hefei National Laboratory for Physical Sciences at Microscale, School of Life  
7 Science, University of Science and Technology of China, Hefei, Anhui 230027,  
8 P.R.China.

9 <sup>c</sup> State Key Laboratory of Brain and Cognitive Science, Institute of Biophysics,  
10 Chinese Academy of Sciences, Beijing 100101, P.R.China.

11 <sup>d</sup> Anhui Province Key Laboratory of Affective Computing and Advanced Intelligent  
12 Machine, School of Computer Science and Information Engineering, Hefei University  
13 of Technology, Hefei, P.R.China

14 <sup>e</sup> current affiliation: NEUROPSYPHY Tzvetomir TZVETANOV EIRL, Horbourg-  
15 Wihr, France & Ciwei Kexue Yanjiu (Shenzhen) Youxian Gongsi 赐为科学研究 (深  
16 圳) 有限公司, P.R.China

17 # corresponding authors

18 **Abstract:**

19 Visual context modulates perception of local orientation attributes. These spatially  
20 very localised effects are considered to correspond to specific excitatory-inhibitory  
21 connectivity patterns of early visual areas as V1, creating perceptual tilt repulsion and  
22 attraction effects. Here, orientation misperception of small Gabor stimuli was used as  
23 a probe of this computational structure by sampling a large spatio-orientation space to  
24 reveal expected asymmetries due to the underlying neuronal processing. Surprisingly,  
25 the results showed a regular iso-orientation pattern of nearby location effects whose  
26 reference point was globally modulated by the spatial structure, without any complex  
27 interactions between local positions and orientation. This pattern of results was  
28 confirmed by the two perceptual parameters of bias and discrimination ability.  
29 Furthermore, the response times to stimulus configuration displayed variations, that  
30 further provided evidence of how multiple early visual stages affect perception of  
31 simple stimuli.

32 **Keywords:** vision; orientation; centre-surround; local & global context.

33

## 34      **Introduction**

35    When we look at a natural scene, local and global spatial context participates in  
36    creating the final percept. It provides cues regarding figure-ground segmentation,  
37    contour integration, or saliency pop-out [1-8], and nowadays it is largely accepted that  
38    early stages of visual processing are strongly shaped by contextual information [9-13].  
39    The task-relevance of context also affects the activity of early visual cortex by  
40    modulating responses to task-irrelevant contextual information [8,14], while all early  
41    visual areas (V1 to V4) through intra- and inter-area recurrent interactions contribute  
42    at different short time scales for the processing of the visual input and to perception  
43    [15-21].

44    Among the basic features coded in the early visual areas, orientation is crucial. It can  
45    be processed as local luminance modulation, or it can be based upon higher-level cues  
46    such as contrasts or textures [22,23], which are more global forms of orientation  
47    information [24-27].

48    For perception of local orientation, since long it is known that it is strongly influenced  
49    by orientation content of nearby spatial locations [28-31], most frequently creating a  
50    tilt repulsion effect such that the perceived orientation of the target would shift away  
51    from the orientation of the contextual element. It is attributed to lateral inhibition in  
52    V1 between local neurons with non overlapping receptive fields [30,32], and  
53    conversely the attractive effects to excitatory interactions. Although other approaches  
54    are proposed [33-35], typically lateral connections in V1 are modelled with a specific  
55    “association field” structure [2,4,7] where excitatory and inhibitory connections are  
56    spatially segregated (Fig.1a-b) and differentially contribute to grouping/segregation of  
57    contour elements. This V1 connectivity pattern is also supported by physiological  
58    studies [5,17].

59    Earlier psychophysical reports of the tilt repulsion effect showed that it is spatially  
60    spread around the centre stimulus [31,32], and the repulsion amplitude was a complex  
61    result of distance, relative orientation between stimuli, and spatial configuration. We  
62    asked whether the spatial excitatory/inhibitory connectivity structure, probed in the  
63    context of the psychophysical tilt illusion paradigm with briefly presented small  
64    stimuli [29-32,36], has any systematic asymmetric spatio-orientation structure as  
65    partially reported [5]. In this later work, Kapadia et al. provided combined  
66    psychophysical and physiological evidence that nearly colinear line segments have  
67    orientation attractive effects corresponding to surround excitatory effects onto  
68    neuronal activity and conversely side-by-side nearly parallel flanks induce repulsive

69 effects. This effect was mainly located within target's close vicinity and they  
70 measured only a limited set of spatial and orientation combinations (e.g. 2D map of  
71 spatial effects for a fixed centre-surround orientation difference).

72 FIGURE 1 HERE

73 Therefore, we set to use the centre-surround tilt illusion effect as a putative probe of  
74 localised V1 lateral interactions by measuring the tilt effect of nearby flanking Gabor  
75 patches onto the central target Gabor stimulus (Fig.1c). We aimed to measure a more  
76 complete map of spatio-orientation interactions of local context onto target's  
77 perception in order to extract a plausible asymmetric spatio-orientation tilt repulsion  
78 (Fig.1d) that should be reminiscent of V1's lateral interaction patterns (Fig.1b). The  
79 results were unexpected and interesting. They made us analyse further the collected  
80 behavioural data that led us to interpret the effects of contextual interactions on  
81 perception with regard to the recent important advances about lateral and feedback  
82 interactions in early visual areas [11,16,18-20,37].

## 83 Results

84 We asked subjects to report the tilt direction of the central Gabor patch (Fig.1c) and  
85 extracted the orientation which each person perceived as vertical under a given local-  
86 global configuration. This was performed for a large range of flank local orientations  
87 and their global positions (Fig.1c, for 12 flank orientations  $\theta_l = \pm 10^\circ, \pm 20^\circ, \pm 40^\circ,$   
88  $\pm 60^\circ, \pm 80^\circ, 0^\circ$ , and  $90^\circ$ , and 8 global positions  $\theta_e = \pm 15^\circ, \pm 30^\circ, \pm 60^\circ, 0^\circ$ , and  $90^\circ$ ; data  
89 collected across multiple blocks of measures; see Methods). Figure 2a-e depicts the  
90 perceived vertical orientation of the central target patch as a function of the local  
91 orientation of the flanks (abscissa) and the global positioning of the three stimuli (also  
92 called envelope; one per panel; all local and global orientations are expressed with  
93 respect to the target orientation; vertically symmetric pairs were pooled for ease of  
94 visualisation). The grey areas depict quadrants where results could be interpreted as  
95 repulsion effects due to local contextual effects. While there were differences in local  
96 contextual modulation, in particular when comparing flanks located at  $60^\circ$  to the other  
97 conditions, we observed a striking regularity in the data. There was a repetitive  
98 pattern of flank orientation effects on perceived values across all their global  
99 locations, with the latter simply shifting vertically the reference point for local effects.  
100 This local orientation "repulsion" is with respect to the mean perceived orientation  
101 (Figure 2, red dashed lines, compare to grey areas), which is computed as the value of  
102 target orientation perception when the flank orientation is  $0^\circ$ , that is parallel to the  
103 target. In contrast, the global position adjusted the global reference point by attracting

104 the perceived local target orientation toward the global orientation. **One can further**  
105 **observe a small angle attraction or no effect for flank orientations of 10° (for**  
106 **similar results see [36], their Fig.4a), but astonishingly this effect seemed present**  
107 **across all envelope positions (cubic-like data variations around flank=0° for few**  
108 **individual curves).** These observations in the data were confirmed by the two-way  
109 analysis of variance that tested the effects of local and global factors (local:  $F(11,66, \hat{\epsilon})$   
110  $=0.333)=25.01, p<0.0001$ ; global:  $F(7,42, \hat{\epsilon}=0.934)=13.84, p<0.0001$ ; interaction:  
111  $F(77,462, \hat{\epsilon}=0.100)=1.53, p=0.175$ ).

112 A post-hoc power and effect size analysis confirmed in our data the strong local effect  
113 (power  $1-\beta>0.999$ , partial  $\eta^2=0.81$ , max standardised difference  $d=7.96, n=7$ ), as  
114 expected from the known fact that local effects on misperception are strong even  
115 within subjects. The same was found for the global positioning effect onto local  
116 perception ( $1-\beta>0.999$ , partial  $\eta^2=0.70, d=5.71, n=7$ ). This modulation by global  
117 position is known [25], but in a configuration with full envelope that covers all local  
118 orientations along the envelope axis, thus creating an oriented and continuously  
119 textured pattern (Fig.1e). Replotting this specific data ( $\theta_{fl}=0^\circ$ ) together with our  
120 control measures of a stimulus with a full elongated Gaussian envelope shows that the  
121 main qualitative effect of the global configuration, whether called position or  
122 orientation, is very similar irrelevant of the stimulus types (Fig.2f). Last, for the  
123 interaction term the observed power of  $1-\beta=0.60$  and effect sizes of partial  $\eta^2=0.20$   
124 and  $d=1.84$  with  $n=7$  subjects hint to weak differences across levels of local-global  
125 orientations that might have been hidden by the limited number of subjects and study  
126 design. To backup this interaction analysis, we asked the converse question of what is  
127 the minimum interaction effect size that we could have detected given our original  
128 hypothesis and current observations. The main hypothesis was that we should see a  
129 switch in bias due to local flank orientation across different surround positions  
130 (Fig.1), i.e. at best opposite effects and at worst a simple amplitude change.  
131 Therefore, we used the data assuming the total mean flank effect and modulated it  
132 between -1 and 1 at location of 0° (-1 total opposite effect, +1 no effect) and linearly  
133 between 0° to 90° spatial locations, the later one being unchanged (by keeping the  
134 individual subjects errors and global effect). This a posteriori analysis showed that  
135 this interaction could have been detected starting from an amplitude decrease of ~40%  
136 between 90° to 0° that corresponds to bias decrease of ~1.6° (~0.92 normalised to

error standard deviation)(see also Supporting Information for the different statistical approach of Bayesian repeated measures ANOVA).

FIGURE 2 HERE

The lack of strong interactions between local orientation and global position, especially on a qualitative basis of opposite tilt effects for excitation and inhibition, was unexpected given the literature reports in psychophysics, physiology of V1, and computational modelling about asymmetrical spatio-orientation interactions and connectivity. Our psychophysical results, with a larger sampling of the spatial and orientation domains, provided an interesting and much simpler picture about perceptual outcomes of centre-surround interactions measured with brief small localised stimuli than previously reported. Local and global contexts acted independently onto perception of the central local orientation.

How can we connect these outcomes to the knowledge that contextual effects onto perception of small stimuli allows to measure and extract local interactions reminiscent of early stages of visual processing? We interpreted our results as follows. Local flanks activated local spatio-orientation inhibitory interactions that created a local repulsion effect onto target tilt perception that is iso-orientation in the spatial domain; the global configuration of the stimuli activated a larger, more global, mechanism whose main effect was to shift the whole local interaction pattern, effect to a large extent independent of the local interaction pattern.

We searched further evidence in our data about this interpretation. It came from the discrimination ability changes of the subjects, here orientation thresholds, as a function of the local-global configuration. These thresholds represent the necessary amount of change in target orientation in order to reliably report its deviation from the perceived vertical. It is known that if the perceptual outcome is based on a maximum likelihood extraction from the neuronal population activated by the stimulus and feature of interest, the best discrimination value, or equivalently threshold, about the stimulus of that neuronal population can be computed [38-40]. Thus, there is also a mechanistic explanation of contextual effects onto thresholds, where it is known that both variables are affected by context and can be correlated [36,41-44]. The results of our subjects for local orientation thresholds are depicted in Figure 3a-e, and show how flank orientation affected thresholds across any global position. **It can be seen that mainly flank orientations of 10°, 20° and 30° increased subjects thresholds (the two configurations of collinear ( $\theta_f=\theta_e=0^\circ$ , Fig.3a) and parallel ( $\theta_f=0^\circ, \theta_e=90^\circ$ , Fig.3e) Gabor patches show strong improvements in thresholds which we associate to these two very specific configurations).** On the contrary, there was no

clear visible effect of global configuration. These observations were confirmed by the two-factor ANOVA analysis on orientation thresholds (local:  $F(11,66, \tilde{\epsilon}=0.267)=5.36$ ,  $p=0.0086$ ; global:  $F(7,42, \tilde{\epsilon}=0.722)=1.52$ ,  $p=0.21$ ; interaction:  $F(77,462, \tilde{\epsilon}=0.141)=1.06$ ,  $p=0.41$ ). The post-hoc power and effect sizes for the local effect were  $1-\beta=0.86$ , partial  $\eta^2=0.47$  and  $d=2.61$ , which we consider as a medium effect of flank orientation given the observed variability. The interaction term gave an F value of 1.06, for which it is impossible to find realistic parameters to obtain significant effect at 0.05 level (experimentally realistic degrees of freedom for numerator and denominator). Given the experimental design, data analysis and observed outcome statistical power for detecting interactions in thresholds seems to necessitate very specific design and data. From another perspective, given the literature reports of correlations between biases and thresholds ([36,41,42,44] ) and the lack of interactions in the previous bias analysis (or at least a weak one not detected by our design), we consider that thresholds should also have weak interactions, but whose magnitude is much smaller than the main local flank effects. Thus, we concluded that local context affected thresholds to a large extent independently from the global configuration, in an equivalent manner as for perceived value.

FIGURE 3 HERE

While these analyses gave information about perceptual changes due to context, we asked whether we can use the behavioural results to further our knowledge about the time course of processing of these interaction patterns. Since local and global levels interact through different levels at short time scales, as demonstrated for example within- and between-areas for the built-up of contours, surfaces or proto-objects [13,16,19,21], we should be able to observe correlates of differential time processing of global and local domains within the behavioural data.

For that purpose we analysed the response times (RTs) of the participants. RTs represent the time the subject took to report their decision about target tilt. For simple RTs as in discrimination and detection experiments they contain three continuous levels of processing: stimulus processing, decision level processing, and motor output processing [45-47]. Since for small localised objects, coding and perception of their orientation is assumed to be mainly affected by interactive feed-forward, lateral and feed-back interactions within and between V1 to V4 areas due to activation by local and global stimulus levels, a delay or speed-up of some condition should be visible in the response times due to time delays in coding the local target orientation. Figure 4

presents the results for mean RTs of our seven participants. Despite the variability of this measure local-global context affected RTs. Flanks local orientation had a main effect (local:  $F(11,66, \tilde{\epsilon}=0.471)=2.76, p=0.034$ ) while global configuration had no significant effect (global:  $F(7,42, \tilde{\epsilon}=0.746)=0.93, p=0.47$ ). Interestingly, the amount of local effects was modulated across global positions (interaction:  $F(77,462, \tilde{\epsilon}=0.192)=1.86, p=0.039$ ), and it can be seen as an asymmetrical RTs data for envelopes of  $30^\circ$  and  $60^\circ$  (Fig.4c,d). This interaction effect was astonishing as the two previous variables had not such an outcome. We extracted the observed power and effect sizes for the interaction term, which were  $1-\beta=0.91$ , partial  $\eta^2=0.24$  and  $d=3.03$  that we consider as medium post-hoc power and effect sizes. To cross-check this significant interaction effect, especially because of the experimental design and global within-subject analysis of variance applied here, we tested each individual block of measure for presence of interactions between local and global orientations (see Methods). From the 58 individual blocks of measures, 10 had significant interaction effect at  $\alpha=0.05$  level, which is unlikely for a binomial distribution with mean 0.05 and  $N=58$  ( $p=0.00056$ ). These 10 significant blocks were distributed among the 7 subjects such that 6 participants had at least one experimental block with significant interaction at  $\alpha=0.05$  level, which corresponds to a population prevalence of 0.85 (with 96% highest posterior density interval of  $[0.48,0.99]$ , see [48,49]; 1 subject with 4/8 significant blocks, 1 subject with 2/8, 3 subjects with 1/8, 1 subject with 1/10, and one with 0/8)(see also Supporting Information - speed accuracy trade off and interaction effects). Thus, it is concluded that the RTs modulation across local-global configuration that was uncovered is significant, though just strong enough to be unexpectedly detected in our study.

FIGURE 4 HERE

## Discussion

Overall, our aim was to investigate the local contextual effects of orientation stimuli onto small and briefly presented orientation targets by sampling a larger spatio-orientation stimulus space. The hypothesis was that such stimulus design probes local primary visual cortex interaction patterns [5,13,30-32,36,50-53] that has a specific excitatory-inhibitory asymmetry (Fig.1). The results revealed that perception of localised target orientation is affected by two levels of contextual information, local

and global, with their effects largely dissociable on local orientation perception. The modulation by local orientation context had an iso-orientation structure in the spatial surround and the envelope orientation modulated these interactions in a global manner without visible local-global interactions.

The above results are at odds with the “association field” hypothesis (Fig.1a,b), where strong spatial segregation is present between excitatory and inhibitory interactions. It predicts opposite tilt illusion effects with spatially segregated attraction/repulsion effects, which was not observed experimentally. It has long been known that tilt repulsion is somehow spread in surround locations [5,31], while its amplitude depended on the specific location and relative orientation of the contextual elements. Our results also demonstrated this, but the more detailed spatio-orientation mapping allowed us to show that these peculiar findings are due to a much simpler interaction than what could be previously considered. Once the global contextual configuration is taken into account the local orientation interactions follow a very simple iso-orientation pattern independent of the global context, which was confirmed by analyses of both perceptual variables of bias and discrimination ability. To some extent, this outcome seems in accord with other studies [54,55] that investigated plausible tilt repulsion asymmetries in the spatial vicinity.

Our findings of the systematic influence of the envelope orientation structure on local orientation perception are in line with previous reports [25]. Processing of global orientation, texture, or real and illusory contours is now accepted to be strongly influenced from post-V1 levels of the visual system where neuronal receptive fields sense a much larger visual space [15,16,18,22,23,27,56]. Importantly, this more global information is sent back to earlier areas and modulates the initial wave of V1’s visual activation [16,19-21], and through dynamic interactions enhances relevant information, or respectively suppresses irrelevant one. These interactions depend on the exact stimulus features that activated local and global V1 to V4 networks, and thus the final outcome is a combination of all processing levels. We propose that the percept formation of small local attributes, which is thought to arise from decoding of V1 neuronal activity, also contains the effects of downstream areas that modulate the V1 responses in a perceptually rather simple manner.

Another important new information from our results, that we think confirms the above interpretation, was the response times modulation of the participants that was depending on the local-global structure. That is, some spatio-orientation configurations of the full stimulus necessitated longer times for the subjects to give their responses. Interestingly, two main effects arose, one from local flank orientation



and one from asymmetrical effects (interactions) across local-global orientations. Thus, we propose that the time to process the stimulus until the final perceptual outcome is differentially affected by the local and global structures. This can be understood if the local RTs modulation is created from local interaction patterns creating the tilt repulsion effect while on top of it comes the effect of the global structure that sets a reference frame. Specifically, we explain the asymmetrical effect by the fact that it happens when contextual local and global orientations are close, and thus, the flank orientations match an expected global elongated spatial structure coded in V2 to V4 that activates a feedback mechanism to V1. Because of the mismatch between the centre target orientation and the global one, this dynamic mechanism adds longer time processing in V1 than other configurations. Interestingly, this time modulation effect across subjects is about 30-50 ms (Fig.4c, d), in the range of V2-V4 feedback effects onto V1 activity reported in recent studies [16,18,19,21,37].

In the analyses presented here, the interest was at investigating the general structure of modulation of orientation perception by orientation context. Whilst the results already provide new important insights, idiosyncratic results are also present between observers (see thin coloured lines in Figures 2-4). The extent of these inter-individual differences and their relation to the early visual processes involved in percept formation [57-61] might provide further important knowledge useful to disentangle neurotypical results in visual perception from conditions due to atypical neural development or ageing [62-64].

In summary, our work provides a renewed understanding of non-invasive probing with small brief stimuli of the early processes of visual input analysis and how they affect the perceptual and behavioural outcomes.

## **DATA AVAILABILITY STATEMENT**

The original contributions presented in the study are included in the article, further inquiries can be directed to the corresponding authors.

## **ETHICS STATEMENT**

The studies involving human participants were reviewed and approved by the Ethics Committee of the School of Life Science (USTC). The participants provided their written informed consent to participate in this study. All data were collected between spring and autumn 2014.

## **AUTHOR CONTRIBUTIONS**

TT and JH designed the experiment and wrote the manuscript. JH collected the data. JH and TT analyzed it. YZ revised the manuscript. All authors contributed to the article and approved the submitted version.

## **ACKNOWLEDGEMENT**

This study was supported by STI2030-Major Projects 2022ZD0204801 (YZ), the Fundamental Research Funds for the Central Universities (TT), the Natural Science Foundation of Hebei Province of China C2019205282 (JH), and the Science and Technology Research Projects of Hebei Normal University L2019B41 (JH).

## **Methods**

### **Observers**

Seven adults (including two of the authors, 3 males), with normal or corrected to normal vision, naive to the purpose of the experiment (with the exception of the two authors), participated in this study. Their age ranged from 23 to 40 years, with an average of  $28.6 \pm 6.3$  (SD). The research protocol followed the guidelines of the Declaration of Helsinki and was approved by the Ethics Committee of the School of Life Science (USTC). Written informed consent was obtained from each participant after explanation of the nature and possible consequences of the study.

### **Apparatus**

All stimuli were displayed on an EIZO FlexScan T962 monitor driven by an NVIDIA Quadro K600 video card and generated by a PC computer running Matlab with PsychToolBox 3 extensions [65,66]. The monitor had a total display area of 40×30 cm, with a resolution of 1920×1440 pixels and a refresh rate of 85 Hz. Participants viewed binocularly the stimuli, which were presented centred on the monitor. A chin-rest was used to minimize subjects' head movements during the experiment. Participants were seated in a darkened room in which all local cues to vertical/horizontal were removed by using black cloth and black cardboard to provide a circular window of 30 cm in diameter to the display [43]. The original 8 bits per pixel luminance range digitization was extended above 10 bits with the contrast box switcher [67], and the monitor weekly calibrated with a custom laboratory automated procedure.

### **Stimuli**

The stimulus consisted of 3 oriented Gabor patches with centres standing in a straight line (Fig.1c). The centre Gabor patch was the target. The two bilateral patches are called flanks and their orientation with respect to the centre patch define the local contextual information. The whole stimulus orientation, that is the straight line going through the three patches centres, which we call the envelope, defined the global contextual information. These angular orientations were defined as  $\theta_c$ ,  $\theta_{fl}$ ,  $\theta_e$ , respectively. We defined centre with vertical orientation as  $0^\circ$  and the two orientations  $\theta_{fl}$ ,  $\theta_e$  are expressed relative to  $\theta_c$ . Positive values express clockwise tilts from the reference. The luminance profile  $L(x,y)$  of the stimulus was computed as follows:

$$\begin{cases} L(x, y) &= L_0 + L_0 C (G_c + G_{fl1} + G_{fl2}) \\ G_c &= \cos(2\pi f X_c) \times \exp(-(x^2 + y^2)/\sigma^2) \\ G_{fl1} &= \cos(2\pi f X_{fl1}) \times \exp(-(x_{fl1}^2 + y_{fl1}^2)/\sigma^2) \\ G_{fl2} &= \cos(2\pi f X_{fl2}) \times \exp(-(x_{fl2}^2 + y_{fl2}^2)/\sigma^2) \end{cases} \quad (1)$$

where  $L_0$  is the mean background luminance of the screen, 30 cd/m<sup>2</sup> in our experiment;  $C$  is the Gabor patch contrast, Michelson contrast, which was fixed at 50% during the experiment;  $f$  is the spatial frequency of the Gabor patches, 4 cycles per degree;  $\sigma$  defines the spatial spread ( $\sigma \sim 1.414 \times$  standard deviation of a classic Gaussian function) of the Gabor patches in both  $x$ - and  $y$ -directions, fixed at  $0.17^\circ$ ;  $(x,y)$  are the spatial coordinates with respect to the central Gabor patch's centre, the target;  $(x_{fl1}, y_{fl1})$  and  $(x_{fl2}, y_{fl2})$  are the flanks' centred coordinates of the two contextual Gabor patches, respectively (see equations below);  $X_c$ ,  $X_{fl1}$ ,  $X_{fl2}$  are the cosines coordinates of the respective Gabor patch for a given orientation (see below); distance between centres of flanks to the central stimulus was defined in wavelength's units as  $d\lambda$  and we used  $d=3$  [50,68]. The terms in equation (1) are defined as:

$$\begin{cases} x_{fl1} &= x + (d\lambda) \cos(\theta_e + \theta_c) \\ y_{fl1} &= y + (d\lambda) \sin(\theta_e + \theta_c) \end{cases} \quad (2)$$

$$\begin{cases} x_{fl2} &= x - (d\lambda) \cos(\theta_e + \theta_c) \\ y_{fl2} &= y - (d\lambda) \sin(\theta_e + \theta_c) \end{cases} \quad (3)$$

$$\begin{cases} X_c &= x \cos(\theta_c) + y \sin(\theta_c) \\ X_{fl1} &= x_{fl1} \cos(\theta_c + \theta_{fl}) + y_{fl1} \sin(\theta_c + \theta_{fl}) \\ X_{fl2} &= x_{fl2} \cos(\theta_c + \theta_{fl}) + y_{fl2} \sin(\theta_c + \theta_{fl}) \end{cases} \quad (4)$$

The parameters  $C=0.5$ ,  $f=4$ ,  $\sigma=0.17$  and  $d=3$  were chosen according to previous

studies [5,36,42,50,68], with the aim of measuring the local spatio-orientation interactions for clearly visible (sufficiently high contrast), frequency band-limited, relatively small ( $f=4\text{cpd}$ ), spatially segregated stimuli. Additionally, the experimental design probed the spatial vicinity of the target location, as it is now accepted to be the major contributor to tilt effects (e.g. [31,54,55]).

For the target stimulus orientation  $\theta_c$ , we denote the vertical orientation as  $0^\circ$ , orientations clockwise (CW) and anti-clockwise (ACW) from vertical or target orientation as positive and negative, respectively. There were 12 orientations  $\theta_f$  ( $\pm 10, \pm 20, \pm 40, \pm 60, \pm 80, 0$ , and  $90$  degrees) for the flanks, and 8 orientations  $\theta_e$  ( $\pm 15, \pm 30, \pm 60, 0$ , and  $90$  degrees) for envelope. We re-emphasise that all flank and envelope orientations are relative to the target.

## Procedure

All seven subjects took part in the whole experiment. They were instructed to fixate a small black square displayed at the centre of the screen and that the stimuli would be briefly presented centred on it. Breaks were set-up in the middle of the experiment to prevent excessive fatigue. They initiated one trial with a key press, then the fixation dot in the middle of the monitor would disappear, and after 235 ms the stimulus would appear and last for 35 ms (see Figure 1e for illustration of timing). Subjects were instructed to focus on the target and respond with two fingers by using two predefined keyboard keys whether the target was clockwise (CW; right arrow key) or **counter-clockwise** (CCW; left arrow key) from their internal vertical standard. They were given 100 practice trials to get used to the task and experiment. The blocks were run in random order across subjects.

This procedure corresponds to the Method of Single Stimulus presentation, where it is assumed that the subject uses a clearly defined internal reference (e.g. obtained from instructions and practice trials; [5,69]) and responds following the instructions.

Though this methodology has gained some criticism about the exact nature of the measured bias (e.g. response bias, perceptual bias, reference bias; e.g. [70,71]), we concur and are in line with the opinion of part of the researchers that, since one can self-experience the perceptual illusion of tilt, the main measure obtained with our design is one of sensory nature, i.e. a perceptual bias [72]. Therefore, we consider the midpoint of the psychometric function as “the perceived (vertical) orientation of the target” for a given configuration.

Simple adaptive testing with the weighted up-down staircase method [73] were used to sample the psychometric function. For each condition, we sampled each psychometric function by varying target orientation with steps Up/Down of  $1/3$  and

3/1 degrees, or 0.5/1.5 and 1.5/0.5 degrees, corresponding to convergence points of 25% and 75%. Staircases started at the opposite side of the convergence point allowing rapid measures within the transition region of the psychometric function. The full experiment was carried in 8 blocks for all but one author subject. In each block we measured 12 conditions ( $2\theta_e \times 6\theta_f$  or  $6\theta_e \times 2\theta_f$ ) (e.g.  $\theta_e = -30^\circ, +30^\circ$ , and  $\theta_f = -80^\circ, -40^\circ, -10^\circ, +10^\circ, +40^\circ, +80^\circ$ ), by selecting orientations for both envelope and flank such that each pair has its vertically symmetric version within each block (see Table 1). There were 40 trials per condition  $\{\theta_e, \theta_f\}$  (each staircase was assigned 20 trials), giving a total of 480 trials per block, and 3840 total trials per subject. One of the author subject ran the experiment with 10 blocks with a different flank-envelope assignment (that included envelope of  $\pm 40^\circ$ , not presented in the results), but keeping the within-block symmetry. Within one block all 24 staircases were presented in a pseudorandom order. All subjects finished the whole experiment within 3-4 days of measurements, coming when they were available, sometimes with days between measures. The blocks were ran in different order across subjects.

## 418 Data Analyses

Maximum likelihood estimation [74] was used to adjust an ad-hoc psychometric functions to each condition  $\{\theta_f, \theta_e\}$ . We fit a 1D psychometric function to the orientation discrimination data for each condition, with probability of CW responses to target orientation  $\theta_c$  given by:

$$423 \quad P(\theta_c) = \lambda + \frac{1-2\lambda}{1+\exp(-\log(21/4)(\theta_c-a)/\sigma)} \quad (5)$$

where here  $\lambda$  is subject's lapsing rate, and  $a$  and  $\sigma$  are the perceived vertical orientation and the threshold of the subject for perceiving a deviation from verticality, respectively. The lapsing rate was fixed at 1% for all subjects. For positive biases ( $a > 0$ ) the perceived orientation of the target as being vertical is CW from the real vertical line, and vice versa. Bias values were adjusted per block by subtracting the mean of the within-block conditions' biases to eliminate internal vertical bias differences across block measures within-subjects, and also between-subjects.

For plot purposes only, as in previous research [5], the data for symmetric envelope orientations of  $\theta_e = \pm 15^\circ, \pm 30^\circ, \pm 60^\circ$  were pooled as follows:

$$433 \quad a(\theta_{fl}, \theta_e) = (a(\theta_{fl}, \theta_e) - a(-\theta_{fl}, -\theta_e)) / 2 \quad (6)$$

$$434 \quad \sigma(\theta_{fl}, \theta_e) = (\sigma(\theta_{fl}, \theta_e) + \sigma(-\theta_{fl}, -\theta_e)) / 2 \quad (7)$$

Response times (RTs) were recorded at millisecond precision and defined as response key press with respect to trial initiation. All RTs were first log-transformed, and then each value was computed and adjusted for within-subject variability as follows: (1) each block RTs were pruned by eliminating any value above  $4 \times rsd$  from block median value (robust estimate of standard deviation:  $rsd(x) = 1.4826 \times \text{median}(|x - \text{median}(x)|)$ ; this eliminated between 2 to 31 values across all 58 blocks, mean of 12), (2) within each block the individual left/right RT were adjusted to the within block mean by taking out the corresponding mean block left/right RTs, (3) each condition  $\{\theta_l, \theta_e\}$  mean RT was computed (based on 34 to 40 values, mean 39), and (4) each individual block of measures mean RT was adjusted to the global mean RT of that subject across all blocks of measures. For plot purposes only, RTs were pooled for symmetric envelope conditions, as for thresholds in equation (7). It should be noted that given the original experimental design with symmetric  $\{\theta_e, \theta_l\}$  measures within a given block and different conditions across blocks of measure, if RTs are modulated across local or global orientations the main effect of step (4) would be to decrease the amount of differences observed across blocks of measures, that is, across local-global configurations measured in different blocks.

## Statistics

Two way within-subject ANOVA was used to analyse whether the two factors local (flank orientation, 12 levels) and global (envelope, 8 levels) influenced the variables extracted about the centre target and whether there was interaction. We performed the two-way ANOVA on biases, thresholds, and log-transformed response times. All statistical levels were Huynh-Feldt epsilon-tilde adjusted;  $p < 0.05$  is considered significant. We further report post-hoc, or observed, power ( $1 - \beta$ ) and post-hoc effect size through the variables partial  $\eta^2$ , which measures the size of the effect given the error variance within the tested effect in the ANOVA, and the maximum standardised difference effect size “d” defined as  $d = (\text{largest difference in means within the tested effect}) / (\text{pooled standard deviation for the effect})$ . The RTs were also analysed at individual subject level within each block of measure for the presence or not of interaction effect between local and global factors; the block RTs that passed the preprocessing were used in a 2-way between-subject ANOVA with the corresponding levels for local and global factors of the given block (see Table 1). We would like to note that this last test has disadvantages in comparison to within-subject designs, and this later design was not carried at individual participant level in the current study.

**Details for measures with an elongated Gaussian envelope (similar to Dakin et al (1999) [25]).**

471 We repeated the design of Dakin et al. (1999) which allowed us to compare the  
 472 similarity between single “envelope” orientation effects and our 3 stimulus design.  
 473 Here, 11 subjects participated (6 males,  $24.1 \pm 5.5$ (SD), 3 subjects also ran the main  
 474 experiment). The stimulus was a cosine grating whose contrast was modulated by a  
 475 single elongated Gaussian envelope as follows:

$$476 \quad \begin{cases} L(x, y) &= L_0 + L_0 C \cos(2\pi f X_c) \times \exp(-x_e^2/\sigma_x^2 - y_e^2/\sigma_y^2) \\ x_e &= x \cos(\theta_c + \theta_e) + y \sin(\theta_c + \theta_e) \\ y_e &= -x \sin(\theta_c + \theta_e) + y \cos(\theta_c + \theta_e) \end{cases} \quad (8)$$

477 with a ratio  $\sigma_y / \sigma_x$  of 3, and  $X_c$  is defined in equation 4. The task of the subject was to  
 478 judge whether the inner central part of the stimulus grating, the “stripes”, was CW or  
 479 CCW from their internal vertical standard; 18 envelope orientations were measured,  
 480 from  $-80^\circ$  to  $90^\circ$  in steps of  $10^\circ$ ; the two staircases sampling a given condition were  
 481 each assigned with 30 trials; this experiment was carried in two blocks, one  
 482 containing the “odd” orientations ( $-70^\circ$  to  $90^\circ$  in steps of  $20^\circ$ ) and the second block  
 483 the remaining “even” orientations (two subjects did not include the  $90^\circ$  envelope due  
 484 to a manipulation error during experimental recording). The remaining experimental  
 485 parameters, design, and procedure were the same as the main experiment. Data  
 486 analysis was similar to the main experiment but with the exception of including a  
 487 prior on the lapse rate, modelled as a single lapse rate within a given block of  
 488 measurement (with prior defined as a Beta probability density function with  
 489 parameters 1.2 and 10). One of the 11 subjects had very high thresholds for envelopes  
 490 near  $0^\circ$ , additionally in about half of the conditions with expected “misperception” the  
 491 biases exhibited opposite signs from the remaining subjects, and finally inspection of  
 492 the individual raw staircases displayed some peculiar raw staircase behaviours. This  
 493 made us suspect that the person did not completely follow the instructions within at  
 494 least one of the blocks. This participant data is not included in Fig.2f.

495

*Table 1: Assignment of flank and envelope conditions to each block of measure for each subject.*

Subject #	Block #	Within block paired orientations of [envelope], [flank]
1	1	[-60 -40 0 40 60 90], [-10 10]
	2	[-60 -40 0 40 60 90], [-20 20]
	3	[-60 -40 0 40 60 90], [-40 40]
	4	[-60 -40 0 40 60 90], [-60 60]
	5	[-60 -40 0 40 60 90], [-80 80]
	6	[-60 -40 0 40 60 90], [0 90]
	7	[-15 15], [-80 -40 -10 10 40 80]
	8	[-15 15], [-60 -20 0 20 60 90]
	9	[-30 30], [-80 -40 -10 10 40 80]
	10	[-30 30], [-60 -20 0 20 60 90]
2, 3	1	[-60 -30 0 30 60 90], [-10 10]
	2	[-60 -30 0 30 60 90], [-20 20]
	3	[-60 -30 0 30 60 90], [-40 40]
	4	[-60 -30 0 30 60 90], [-60 60]
	5	[-60 -30 0 30 60 90], [-80 80]
	6	[-60 -30 0 30 60 90], [0 90]
	7	[-15 15], [-80 -40 -10 10 40 80]
	8	[-15 15], [-60 -20 0 20 60 90]
4, 5, 6, 7	1	[-15 15], [-80 -40 -10 10 40 80]
	2	[-15 15], [-60 -20 0 20 60 90]
	3	[-30 30], [-80 -40 -10 10 40 80]
	4	[-30 30], [-60 -20 0 20 60 90]
	5	[-60 60], [-80 -40 -10 10 40 80]
	6	[-60 60], [-60 -20 0 20 60 90]
	7	[0 90], [-80 -40 -10 10 40 80]
	8	[0 90], [-60 -20 0 20 60 90]

496

497



## 499 References

- 500 1. Nothdurft, H. (1991) Texture segmentation and pop-out from orientation contrast, *Vision*  
501 *Research* 31:1073-1078.
- 502 2. Field, D. J., Hayes, A. and Hess, R. F. (1993) Contour integration by the human visual system :  
503 evidence for a local association field, *Vision Research* 33:173-193.
- 504 3. Nothdurft, H. C. (1994) Common properties of visual segmentation., *Ciba Foundation*  
505 *symposium* 184:245-59; discussion 260-71.
- 506 4. Li, Z. (1999) Visual segmentation by contextual influences via intra-cortical interactions in the  
507 primary visual cortex, *Network: Computation in Neural Systems* 10:187-212.
- 508 5. Kapadia, M. K., Westheimer, G. and Gilbert, C. D. (2000) Spatial distribution of contextual  
509 interactions in primary visual cortex and in visual perception, *Journal of Neurophysiology*  
510 84:2048-2062.
- 511 6. Li, Z. (2002) A saliency map in primary visual cortex, *Trends in Cognitive Sciences* 6:9-16.
- 512 7. Piëch, V., Li, W., Reeke, G. N. and Gilbert, C. D. (2013) Network model of top-down influences  
513 on local gain and contextual interactions in visual cortex, *Proceedings of the National Academy of*  
514 *Science USA* 110:E4108-E4117.
- 515 8. Wagatsuma, N., Oki, M. and Sakai, K. (2013) Feature-Based Attention in Early Vision for the  
516 Modulation of Figure–Ground Segregation, *Frontiers in psychology* 4:123.
- 517 9. Albright, T. D. and Stoner, G. R. (2002) Contextual influences on visual processing, *Annual*  
518 *Review of Neuroscience* 25:339-379.
- 519 10. Kingdom, F. A., Angelucci, A. and Clifford, C. W. (2014) Special issue: The function of  
520 contextual modulation, *Vision Research* 104:1 - 2.
- 521 11. Nurminen, L. and Angelucci, A. (2014) Multiple components of surround modulation in  
522 primary visual cortex: Multiple neural circuits with multiple functions?, *Vision Research* 104:47 -  
523 56.
- 524 12. Schmid, A. M. and Victor, J. D. (2014) Possible functions of contextual modulations and  
525 receptive field nonlinearities: Pop-out and texture segmentation, *Vision Research* 104:57 - 67.
- 526 13. Frégnac, Y. and Bathellier, B. (2015) Cortical Correlates of Low-Level Perception: From Neural  
527 Circuits to Percepts, *Neuron* 88:110-126.
- 528 14. Gilbert, C. D. and Li, W. (2013) Top-down influences on visual processing, *Nature Reviews*  
529 *Neuroscience* 14:350-63.

530 15. Pan, Y., Chen, M., Yin, J., An, X., Zhang, X., Lu, Y., Gong, H., Li, W. and Wang, W. (2012)  
531 Equivalent representation of real and illusory contours in macaque V4., *The Journal of*  
532 *neuroscience : the official journal of the Society for Neuroscience* 32:6760-70.

533 16. Chen, M., Yan, Y., Gong, X., Gilbert, C. D., Liang, H. and Li, W. (2014) Incremental integration of  
534 global contours through interplay between visual cortical areas, *Neuron* 82:682-694.

535 17. Gerard-Mercier, F., Carelli, P. V., Pananceau, M., Troncoso, X. G. and Frégnac, Y. (2016)  
536 Synaptic Correlates of Low-Level Perception in V1., *The Journal of neuroscience : the official*  
537 *journal of the Society for Neuroscience* 36:3925-42.

538 18. Klink, P. C., Dagnino, B., Gariel-Mathis, M.-A. and Roelfsema, P. R. (2017) Distinct Feedforward  
539 and Feedback Effects of Microstimulation in Visual Cortex Reveal Neural Mechanisms of Texture  
540 Segregation., *Neuron* 95:209-220.e3.

541 19. Liang, H., Gong, X., Chen, M., Yan, Y., Li, W. and Gilbert, C. D. (2017) Interactions between  
542 feedback and lateral connections in the primary visual cortex., *Proceedings of the National*  
543 *Academy of Sciences of the United States of America* 114:8637-8642.

544 20. Yan, Y., Zhaoping, L. and Li, W. (2018) Bottom-up saliency and top-down learning in the  
545 primary visual cortex of monkeys., *Proceedings of the National Academy of Sciences of the United*  
546 *States of America* 115:10499-10504.

547 21. Self, M. W., Jeurissen, D., van Ham, A. F., van Vugt, B., Poort, J. and Roelfsema, P. R. (2019) The  
548 Segmentation of Proto-Objects in the Monkey Primary Visual Cortex., *Current biology : CB*  
549 29:1019-1029.e4.

550 22. Zhou, Y.-X. and Baker, C. L. (1993) A processing stream in mammalian visual cortex neurons for  
551 non-Fourier responses, *Science* 261:98-101.

552 23. Zhou, Y.-X. and Baker, C. L. (1994) Envelope-responsive neurons in areas 14 and 18 of cat,  
553 *Journal of Neurophysiology* 72:2134-2150.

554 24. Morgan, M. J. and Baldassi, S. (1997) How the human visual system encodes the orientation  
555 of a texture, and why it makes mistakes, *Current Biology* 7:999-1002.

556 25. Dakin, S. C., Williams, C. B. and Hess, R. F. (1999) The interaction of first- and second-order  
557 cues to orientation, *Vision Research* 39:2867-2884.

558 26. Tanaka, H. and Ohzawa, I. (2006) Neural basis for stereopsis from second-order contrast cues.,  
559 *The Journal of neuroscience : the official journal of the Society for Neuroscience* 26:4370-82.

560 27. Li, G., Yao, Z., Wang, Z., Yuan, N., Talebi, V., Tan, J., Wang, Y., Zhou, Y. and Baker, C. L. J. (2014)  
561 Form-cue invariant second-order neuronal responses to contrast modulation in primate area V2.,  
562 *The Journal of neuroscience : the official journal of the Society for Neuroscience* 34:12081-92.

- 563 28. Gibson, J. J. and Radner, M. (1937) Adaptation, after-effect, and contrast in the perception of  
564 tilted lines. I. quantitative studies, *Journal of Experimental Psychology* 20:453-467.
- 565 29. Georgeson, M. (1973) Spatial frequency selectivity of a visual tilt illusion, *Nature* 245:43-45.
- 566 30. Gilbert, C. D. and Wiesel, T. N. (1990) The influence of contextual stimuli on the orientation  
567 selectivity of cells in primary visual cortex of the cat, *Vision Research* 30:1689-1701.
- 568 31. Westheimer, G. (1990) Simultaneous orientation contrast for lines in the human fovea, *Vision*  
569 *Research* 30:1913-1921.
- 570 32. Blakemore, C., Carpenter, R. H. S. and Georgeson, M. (1970) Lateral inhibition between  
571 orientation detectors in the human visual system, *Nature* 228:37-39.
- 572 33. Grossberg, S. and Mingolla, E. (1985) Neural dynamics of form perception : boundary  
573 completion, illusory figures, and neon color spreading, *Psychological Review* 92:173-211.
- 574 34. Grossberg, S. and Williamson, J. (1999). *A neural model of how horizontal and interlaminar*  
575 *connections of visual cortex develop into adult circuits that carry out perceptual grouping and*  
576 *learning*, .
- 577 35. Raizada, R. and Grossberg, S. (2001) Context-sensitive binding by the laminar circuits of V1  
578 and V2 : a unified model of perceptual grouping, attention, and orientation contrast, *Visual*  
579 *Cognition* 8:431-466.
- 580 36. Solomon, J. A., Felisberti, F. M. and Morgan, M. (2004) Crowding and the tilt illusion: toward a  
581 unified account, *Journal of Vision* 4:500-508.
- 582 37. Chen, R., Wang, F., Liang, H. and Li, W. (2017) Synergistic Processing of Visual Contours across  
583 Cortical Layers in V1 and V2., *Neuron* 96:1388-1402.e4.
- 584 38. Paradiso, M. A. (1988) A theory for the use of visual orientation information which exploits  
585 the columnar structure of striate cortex, *Biological Cybernetics* 58:35-49.
- 586 39. Seung, H. and Sompolinsky, H. (1993) Simple models for reading neuronal population codes,  
587 *Proceedings of the National Academy of Science USA* 90:10749-10753.
- 588 40. Brunel, N. and Nadal, J.-P. (1998) Mutual information, Fisher information, and population  
589 coding, *Neural Computation* 10:1731-1757.
- 590 41. Tzvetanov, T. and Womelsdorf, T. (2008) Predicting human perceptual decisions by decoding  
591 neuronal information profiles, *Biological Cybernetics* 98:397-411.
- 592 42. Solomon, J. A. and Morgan, M. (2009) Strong tilt illusions always reduce orientation acuity,  
593 *Vision Research* 49:819-824.
- 594 43. Tzvetanov, T. (2012) A single theoretical framework for circular features processing in humans:  
595 orientation and direction of motion compared, *Frontiers in Computational Neuroscience* 6.

596 44. Wei, X. X. and Stocker, A. A. (2017) Lawful relation between perceptual bias and  
597 discriminability, *Proceedings of the National Academy of Sciences of the United States of America*  
598 114:10244.

599 45. Luce, R. D. (1986) *Response Times* (Oxford University Press).

600 46. Pins, D. and Bonnet, C. (1996) On the relation between stimulus intensity and processing time  
601 : Piéron's law and choice reaction time, *Perception & Psychophysics* 58:390-400.

602 47. Palmer, J., Huk, A. C. and Shadlen, M. N. (2005) The effect of stimulus strength on the speed  
603 and accuracy of a perceptual decision, *Journal of Vision* 5:376-404.

604 48. Ince, R. A., Paton, A. T., Kay, J. W. and Schyns, P. G. (2021) Bayesian inference of population  
605 prevalence., *eLife* 10.

606 49. Ince, R. A. A., Kay, J. W. and Schyns, P. G. (2022) Within-participant statistics for cognitive  
607 science., *Trends in cognitive sciences* 26:626-630.

608 50. Polat, U. and Sagi, D. (1993) Lateral interactions between spatial channels : suppression and  
609 facilitation revealed by lateral masking experiments, *Vision Research* 33:993-999.

610 51. Spillmann, L. and Ehrenstein, W. (1996) Comprehensive Human Physiology, in ( ed. R. Greger,  
611 U. W.) 861-893 (Springer-Verlag Berlin Heidelberg).

612 52. Dresch, B. (1999) Dynamic characteristics of spatial mechanisms coding contour structures,  
613 *Spatial Vision* 12:129-142.

614 53. Polat, U. (1999) Functional architecture of long-range perceptual interactions, *Spatial Vision*  
615 12:143-162.

616 54. Mareschal, I. and Clifford, C. W. G. (2012) Dynamics of unconscious contextual effects in  
617 orientation processing., *Proceedings of the National Academy of Sciences of the United States of*  
618 *America* 109:7553-8.

619 55. Mareschal, I. and Clifford, C. W. G. (2013) Spatial structure of contextual modulation., *Journal*  
620 *of vision* 13.

621 56. Mareschal, I. and Baker, C. L. (1998) A cortical locus for the processing of contrast-defined  
622 contours, *Nature Neuroscience* 1:150-154.

623 57. Song, C., Schwarzkopf, D. S., Lutti, A., Li, B., Kanai, R. and Rees, G. (2013) Effective connectivity  
624 within human primary visual cortex predicts interindividual diversity in illusory perception., *The*  
625 *Journal of neuroscience : the official journal of the Society for Neuroscience* 33:18781-91.

626 58. Peterzell, D. H. (2016) Discovering Sensory Processes Using Individual Differences: A Review  
627 and Factor Analytic Manifesto., *Electronic Imaging* 2016:1-11.

- 628 59. Bosten, J. M., Mollon, J. D., Peterzell, D. H. and Webster, M. A. (2017) Individual differences as  
629 a window into the structure and function of the visual system., *Vision research* 141:1-3.
- 630 60. Mollon, J. D., Bosten, J. M., Peterzell, D. H. and Webster, M. A. (2017) Individual differences in  
631 visual science: What can be learned and what is good experimental practice?, *Vision research*  
632 141:4-15.
- 633 61. Tulver, K. (2019) The factorial structure of individual differences in visual perception.,  
634 *Consciousness and cognition* 73:102762.
- 635 62. Huang, J., Zhou, Y., Liu, C., Liu, Z., Luan, C. and Tzvetanov, T. (2017) The neural basis of spatial  
636 vision losses in the dysfunctional visual system, *Scientific Reports* 7:11376.
- 637 63. King, D. J., Hodgekins, J., Chouinard, P. A., Chouinard, V.-A. and Sperandio, I. (2017) A review  
638 of abnormalities in the perception of visual illusions in schizophrenia, *Psychonomic Bulletin &*  
639 *Review* 24:734-751.
- 640 64. McKendrick, A. M., Chan, Y. M. and Nguyen, B. N. (2018) Spatial vision in older adults:  
641 perceptual changes and neural bases, *Ophthalmic Physiol Opt* 38:363-375.
- 642 65. Brainard, D. H. (1997) The psychophysics toolbox, *Spatial Vision* 10:433-436.
- 643 66. Pelli, D. G. (1997) The videotoolbox software for visual psychophysics: transforming numbers  
644 into movies, *Spatial Vision* 10:437-442.
- 645 67. Li, X., Lu, Z.-L., Xu, P., Jin, J. and Zhou, Y.-F. (2003) Generating high gray-level resolution  
646 monochrome displays with conventional computer graphics cards and color monitors, *Journal of*  
647 *Neuroscience Methods* 130:9-18.
- 648 68. Tzvetanov, T. and Simon, L. (2006) Short- and long-range spatial interactions: a redefinition,  
649 *Vision Research* 46:1302-1306.
- 650 69. Morgan, M., Watamaniuk, S. N. and McKee, S. P. (2000) The use of an implicit standard for  
651 measuring discrimination thresholds, *Vision Research* 40:2341-2349.
- 652 70. Garcia-Perez, M. A. and Alcala-Quintana, R. (2013) Shifts of the psychometric function:  
653 distinguishing bias from perceptual effects, *The Quarterly Journal of Experimental Psychology*  
654 66:319-337.
- 655 71. Morgan, M. J., Delmoth, D. and Solomon, J. A. (2013) Linking hypotheses underlying Class A  
656 and Class B methods, *Visual Neuroscience* 30:197-206.
- 657 72. Dekel, R. and Sagi, D. (2020) A decision-time account of individual variability in context-  
658 dependent orientation estimation, *Vision Research* 177:20-31.
- 659 73. Kaernbach, C. (1991) Simple adaptive testing with the weighted up-down method, *Perception*  
660 *& Psychophysics* 49:227-229.

661 74. Treutwein, N. and Strasburger, H. (1999) Fitting the psychometric function, *Perception &*  
662 *Psychophysics* 61:87-106.

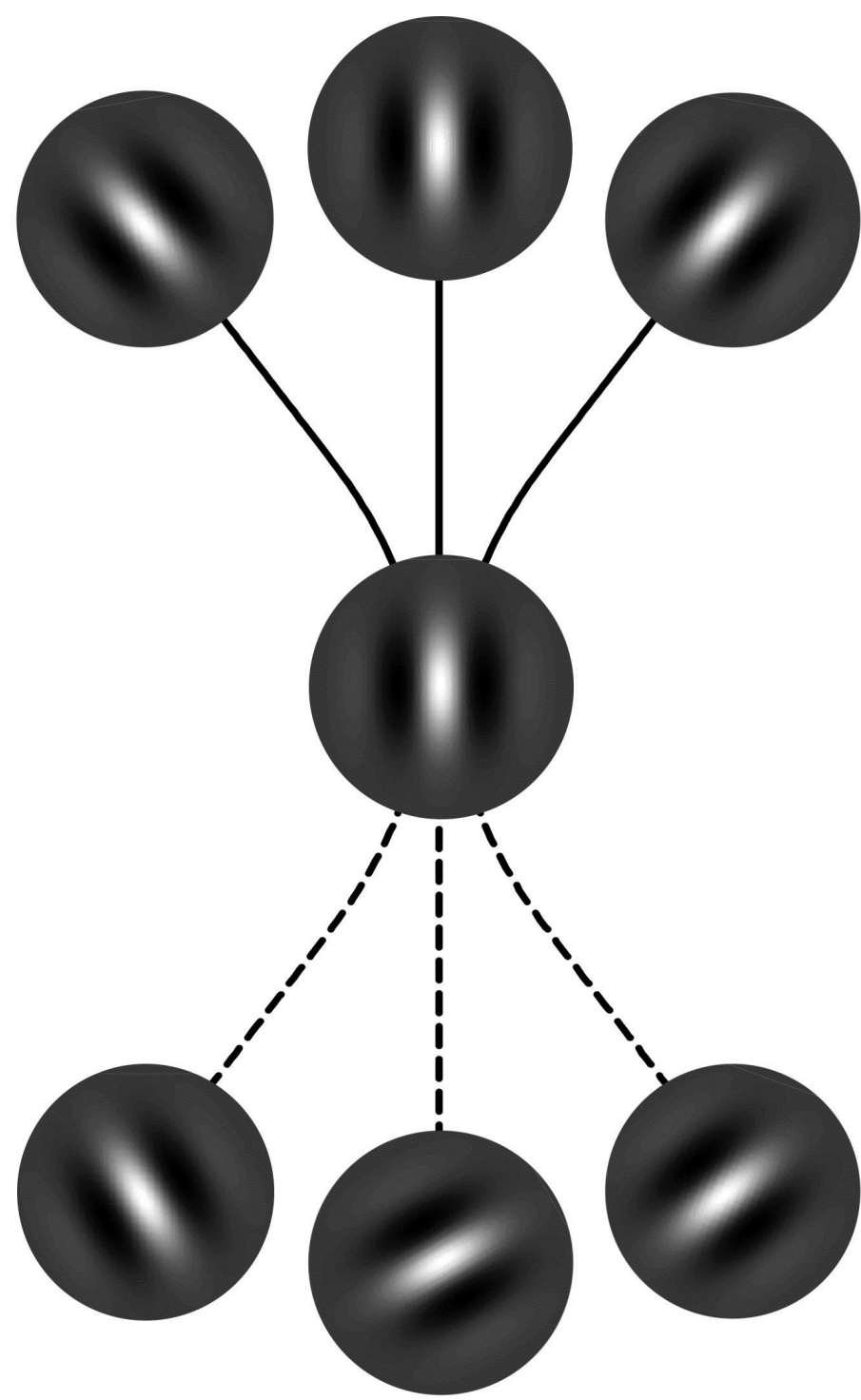
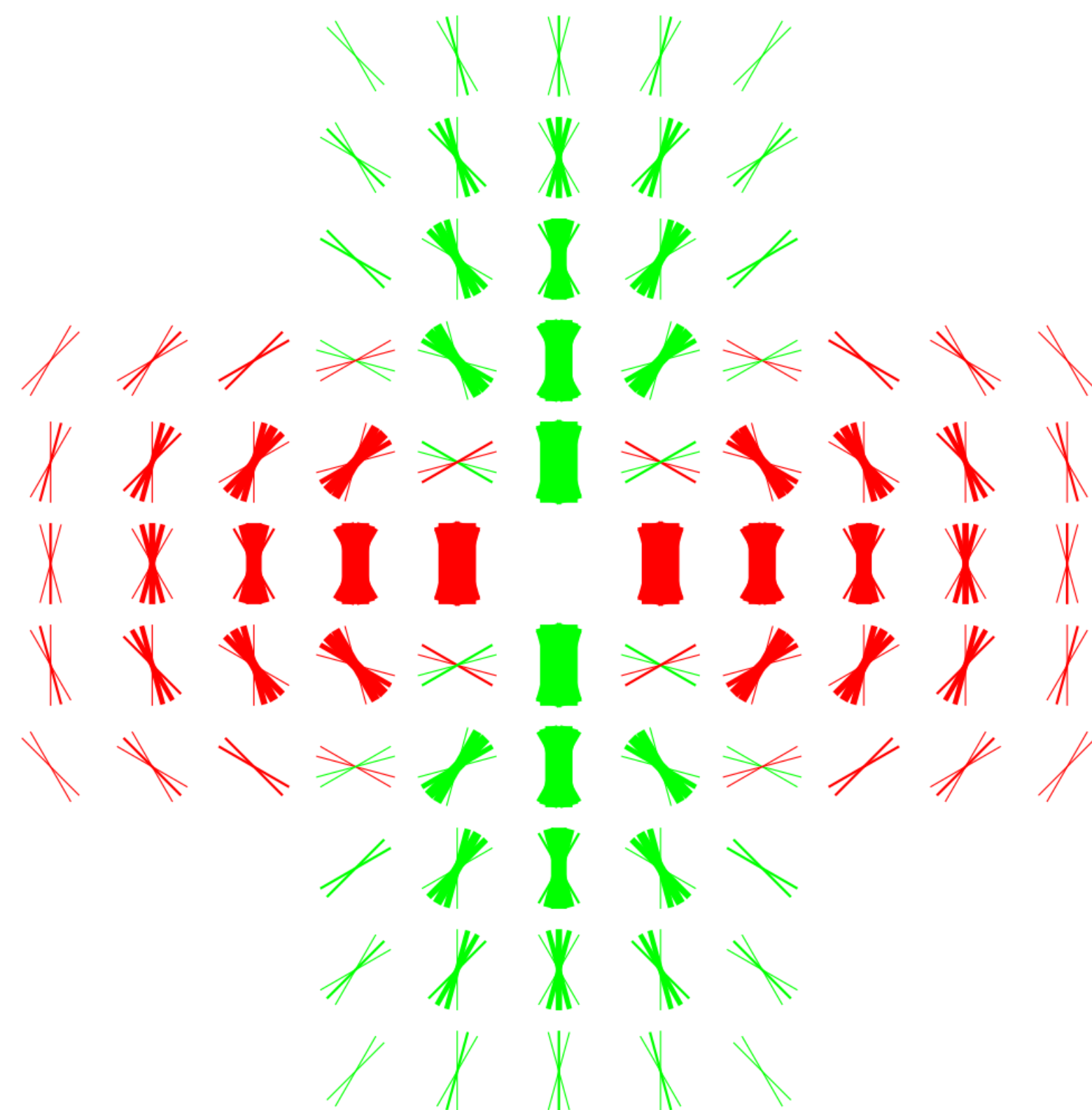
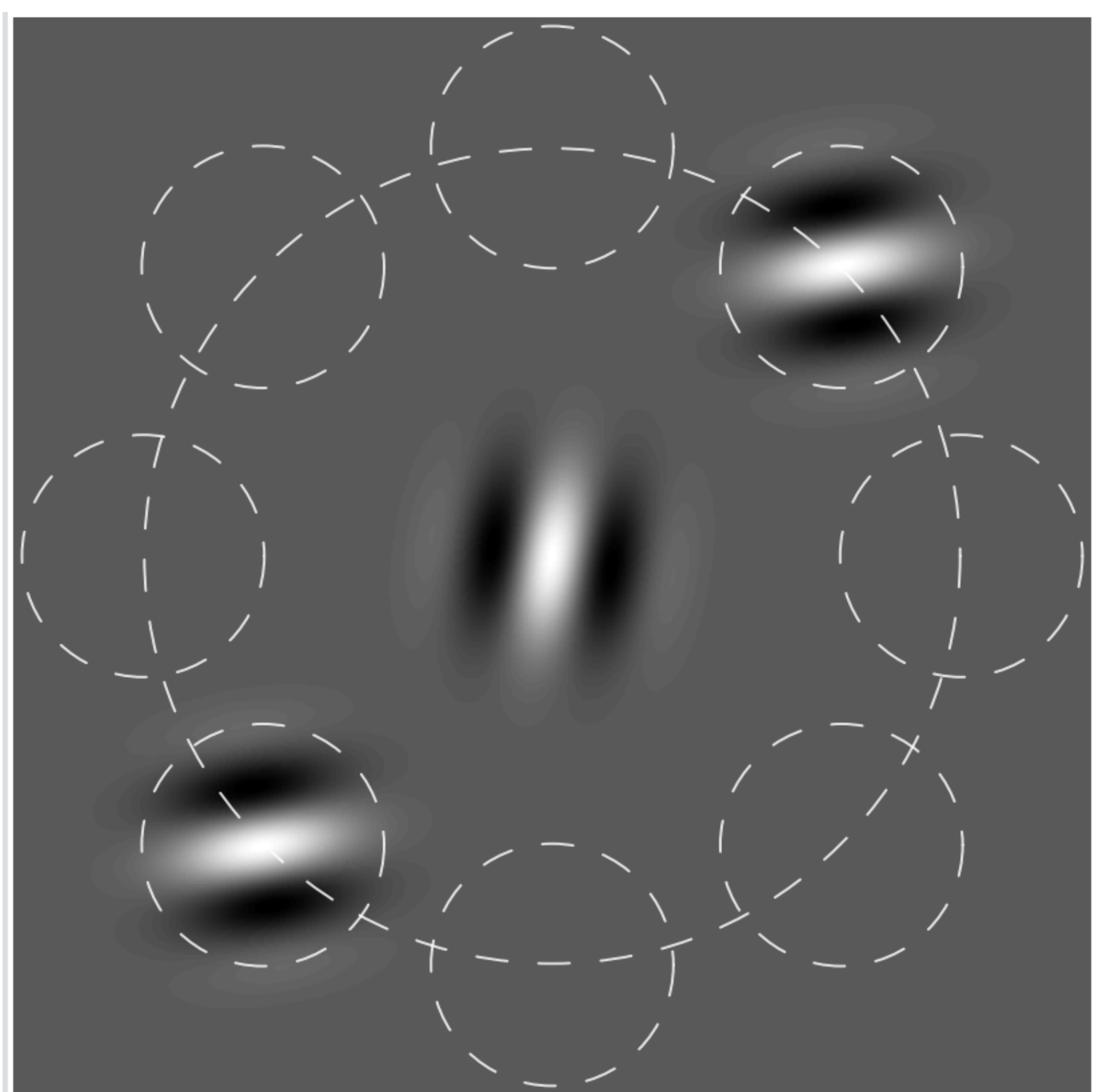
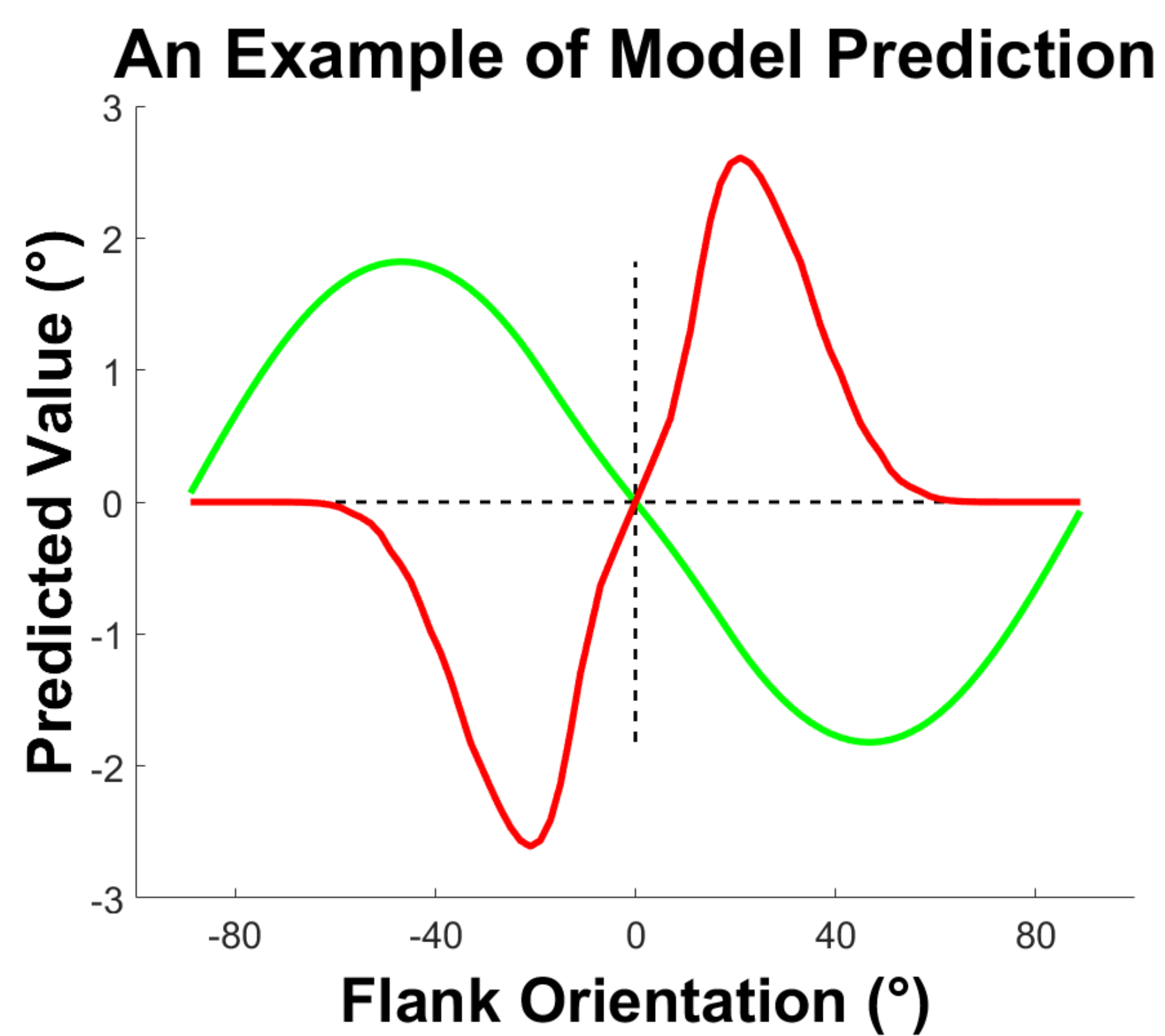
## FIGURE CAPTIONS

Figure 1: Hypothesis. (a) Association field for a vertical preferred element. The elements on the top that have the same orientations as the connection lines, can establish an excitatory connection with the central element. In contrast, the elements with orientations different from the connection lines cannot have a connection with the central element or inhibit it (redraw Figure 16 from Field, Hayes et al(1993)). (b) Excitatory (green) and inhibitory (red) connectivity pattern for a node with a vertical orientation preference as example of implementation of the "association field"(connectivity following model equations of Piech et al (2013)). (c) Illustration of stimulus configuration for measuring the spatio-orientation interactions; small white dotted circles – flanks locations sampled in our measures; large white dotted circle depicts the constant radial flanks distance from the central stimulus; Gabor patches depict a central vertical stimulus flanked by two Gabor patches at  $\theta_e = +30^\circ$  and  $\theta_f = +60^\circ$ . (d) Qualitative illustration of putative opposite orientation tilts for excitatory (green curve; e.g.  $\theta_e = 0^\circ$ ) and inhibitory (red curve, e.g.  $\theta_e = 90^\circ$ ) for a centre of 0 degrees (non cardinal flank positions additionally translate the curves along the x-axis, because the peak of the effect is off the centre orientation). (e) Trial timing and stimulus. The upper and lower grey squares, second from right, respectively, display sample stimuli used in the main experiment and the elongated Gaussian experiment (**red dashed lines depict local orientation and the red arrow the perceived tilt change of the target**).

Figure 2: Results for contextual biases. (a-e) Perceived vertical target orientation as a function of local flank orientation for different envelope orientations ( $n=7$ ). The grey area in each panel represents quadrants interpreted as local repulsion effects for envelopes of  $0^\circ$  and  $90^\circ$ ; red dashed lines help visualise the local reference point of repulsion set by the global envelope configuration. (f) Results for perceived vertical of local orientation as a function of envelope orientation when all local orientations are parallel: our results with 3 parallel Gabor patches replotted from (a-e) (Flank or. =  $0^\circ$ ;  $n=7$ ), and control measures for an elongated Gaussian envelope ( $n=10$ ). Error bars represent between subjects standard errors. In all panels symmetric configurations for opposite sign envelopes were pooled for ease of visualisation. Thin coloured lines are individual subjects results. Black circles and red squares with error bars represent between subjects mean and SEM.

Figure 3: Results for discrimination thresholds. (a-e) Discrimination thresholds of target orientation around perceived vertical as a function of local flank orientation for different envelope orientations. Black circles with error bars represent between subjects mean and SEM ( $n=7$ ). Thin coloured lines are individual subjects results.

Figure 4: Results for response times to target orientation as a function of local flank orientation (abscissa) for different envelope orientations (panels (a-e)). Black circles with error bars represent between subjects mean and SEM ( $n=7$ ). Thin coloured lines are individual subjects results.

**a****b****c****d****e**